# Tumor angiogenesis is caused by single melanoma cells in a manner dependent on reactive oxygen species and NF-κB

**Maximilian K. Schaafhausen[1], Wan-Jen Yang[2,3], Lazaro Centanin[4], Joachim Wittbrodt[4,5], Anja Bosserhoff[6], Andreas Fischer[2,3], Manfred Schartl[1,7] and Svenja Meierjohann[1,7,*]**

[1]Department of Physiological Chemistry I, Biocenter, Am Hubland, University of Wurzburg, Wurzburg, Germany
[2]Vascular Signaling and Cancer, German Cancer Research Center (DKFZ-ZMBH Alliance), Heidelberg, Germany
[3]Vascular Biology, Medical Faculty Mannheim (CBTM), Heidelberg University, Mannheim, Germany
[4]Centre for Organismal Studies, University of Heidelberg, Heidelberg, Germany
[5]Institute of Toxicology and Genetics, Karlsruhe Institute of Technology, Eggenstein-Leopoldshafen, Germany
[6]Institute of Pathology, University of Regensburg, Regensburg, Germany
[7]Comprehensive Cancer Center Mainfranken, University Hospital Wurzburg, Germany
*Author for correspondence (svenja.meierjohann@biozentrum.uni-wuerzburg.de)

*Accepted 6 June 2013*
*Journal of Cell Science 126, 3862–3872*

*doi: 10.1242/jcs.125021*

## Summary

Melanomas have a high angiogenic potential, but respond poorly to medical treatment and metastasize very early. To understand the early events in tumor angiogenesis, animal models with high tumor resolution and blood vessel resolution are required, which provide the opportunity to test the ability of small molecule inhibitors to modulate the angiogenic tumor program. We have established a transgenic melanoma angiogenesis model in the small laboratory fish species Japanese medaka. Here, pigment cells are transformed by an oncogenic receptor tyrosine kinase in fish expressing GFP throughout their vasculature. We show that angiogenesis occurs in a reactive oxygen species (ROS)- and NF-κB-dependent, but hypoxia-independent manner. Intriguingly, we observed that blood vessel sprouting is induced even by single transformed pigment cells. The oncogenic receptor as well as human melanoma cells harboring other oncogenes caused the production of pro-angiogenic factors, most prominently angiogenin, through NF-κB signaling. Inhibiting NF-κB prevented tumor angiogenesis and led to the regression of existing tumor blood vessels.

In conclusion, our high-resolution medaka melanoma model discloses that ROS and NF-κB signaling from single tumor cells causes hypoxia-independent angiogenesis, thus, demonstrating that the intrinsic malignant tumor cell features are sufficient to initiate and maintain a pro-angiogenic signaling threshold.

**Key words:** NF-κB, ROS, Melanoma, Tumor angiogenesis

## Introduction

Angiogenesis, the development of new blood vessels from pre-existing vasculature, is a regularly occurring process in the adult body which takes place e.g. during wound healing or the female menorrhea cycle. Under physiological conditions, angiogenesis is temporally and spatially well-controlled, as pro- and anti-angiogenic factors are strictly regulated. Under pathological conditions, as for example in tumors, an abnormal secretion of some of these factors results in an imbalance of pro- and anti-angiogenic factors, and tumor angiogenesis is favored. This so-called angiogenic switch is an essential step in tumor progression, as only vascularisation of a tumor can guarantee sufficient supply of the tumor cells with oxygen and nutrients, which is the prerequisite for tumor expansion. It has been shown in several transplantation experiments that the size limit of avascular tumors is between 0.2 to 2 mm of diameter (Folkman, 2000). This correlates with the tissue oxygen diffusions limit of ~100 to 200 μm (Gasparini, 1999). When a growing tumor reaches a size larger than two millimeters, cells in the inner mass suffer from low oxygen tension (hypoxia). Hypoxia is one of the best characterized angiogenesis triggers, and it is usually initiated by the stabilization of hypoxia-inducible factor 1 alpha (HIF-1α), followed by the induction of pro-angiogenic factors such as vascular endothelial growth factor (VEGF). However, tumor angiogenesis can also occur under normoxic conditions (Lee et al., 2008).

Among the broad range of human cancers, malignant melanoma, originating from melanocytes, belongs to the most aggressive forms. The incidence of melanoma increases by 3–7% per annum in Caucasian populations. Among the genes which play a critical role in melanoma development and progression are components of the *RAS-RAF-MAPK* signaling pathway, the *PI3K/AKT* pathway and the *CDKN2A* locus.

The knowledge that human melanoma cells are able to induce angiogenesis dates back to the 1960s when Warren and Shubik first discovered that biopsied human melanoma cells transplanted into hamster cheek pouches induce tumor neovascularisation (Warren and Shubik, 1966). Since then, several proangiogenic factors were discovered which play a pivotal role in tumor – including melanoma – angiogenesis. Among these are VEGF, bFGF and IL-8 as well as PlGF, PDGF, and angiogenin (Dutcher, 2001; Hartmann et al.,

1999). Today it is a well-established fact that angiogenesis is essential for progression and metastatic spread of solid tumors. However, the molecular components which contribute to these angiogenic processes are only partly understood.

To date, a broad variety of *in vitro* and *ex vivo* angiogenesis tools and assays are available, such as endothelial cell proliferation, migration and differentiation assays or organ culture assays. These tools are useful for screening potential inhibitors or inducers of angiogenesis and for testing and validating new drugs (Staton et al., 2009). However, they can only give limited information about the pro- and anti-angiogenic interactions that take place in the natural microenvironment. In addition, dosage issues or side effects of new drugs cannot be addressed. Therefore, *in vivo* models are essential to study effects of tumor angiogenesis in the whole organism. Most available *in vivo* models require transplantation or xenotransplantation of tumor cells, and test animals can only be analyzed at the experimental end point, when they are dissected to investigate affected organs or tissues. Some of these problems can be overcome using transparent animals, like the zebrafish (*Danio rerio*) or the Japanese ricefish medaka (*Oryzias latipes*). They produce large numbers of embryos per day with optical clarity and *ex utero* development which facilitate monitoring. With respect to therapeutic strategies, small aquarium fish in particular offer the unique opportunity to perform large scale anti-angiogenic drug testing on whole animals. For zebrafish, several xenotransplantation angiogenesis models do exist (Nicoli et al., 2007; Stoletov et al., 2007). Almost all of them describe the vascularisation after injection of human melanoma or other tumor cells into embryos or larvae. While these models are certainly useful for examining the effects of established tumor cells, they still harbor some intrinsic physiological disadvantages, such as the fact that human cells are transferred to low temperature conditions, which are required for fish maintenance (approx. 26°C), and into a developing environment with unfinished organism vascularisation. We thus aimed at monitoring tumor generation, progression and angiogenesis in adult transparent fish, allowing us to observe the tumorigenic processes in their natural tissue microenvironment with high-resolution bioimaging techniques. We recently developed the *mitf::xmrk* medaka melanoma model (Schartl et al., 2010), where the melanoma oncogene *xmrk*, a fish orthologue of the human EGF receptor, is stably expressed under the pigment cell-specific *mitf* promoter, leading to the formation of pigment cell tumors with an early onset and 100% penetrance. To generate the first transgenic fish tumor angiogenesis model, we crossed these fishes with medakas stably expressing GFP in their vasculature *(fli::egfp)*, thus allowing imaging of the blood vessels. We show that transformed pigment cells have a high capacity to induce hypoxia-independent tumor angiogenesis by activating the NF-κB pathway. *In vitro* experiments confirm the Xmrk-induced and NF-κB-dependent secretion of pro-angiogenic factors. Interestingly, we could demonstrate that human melanoma cells also feature permanent activation of NF-κB, which is accompanied by the secretion of pro-angiogenic factors such as angiogenin. Furthermore these data demonstrate that this angiogenesis model is perfectly suited for long-term monitoring of angiogenesis events in live fish and for the evaluation of small molecule inhibitor efficacy in the whole organism.

## Results

### *mitf::xmrk* fish display strong tumor angiogenesis

To elucidate the tumor angiogenic capacity of melanoma cells, we crossed *mitf::xmrk* transgenic medakas, expressing *xmrk* under control of the pigment cell specific *mitf* promotor, with *fli::egfp* transgenic medakas which express *egfp* under the control of the hemangioblast specific *fli* promotor. This resulted in the generation of melanoma-developing fish with GFP-positive blood vessels. For microscopic analysis, the caudal fin was chosen because it provides a well-structured vascular pattern, and disruption of this pattern by tumor angiogenesis can easily be detected. Furthermore, the transparency of the fin is well-suited for imaging (Fig. 1Ai–ii). In comparison to *fli::egfp* fish (Fig. 1Bi), the melanoma-bearing *fli::egfp;mitf::xmrk* animals displayed numerous transformed pigment cells in the caudal fins, visible as black (melanophore) and yellow (xantho- or erythrophore) spots (Fig. 1Ci). Both pigment cell types are characterized by *mitf* expression, and in *mitf::xmrk* transgenic fish, they both express the oncogene Xmrk (Schartl et al., 2010). Strikingly, the presence of *xmrk*-expressing pigment cells in the fins resulted in a strong increase of angiogenic sprouts compared to control fish (Fig. 1B,C). To quantify changes in vascular patterns among adult *fli::egfp* and *fli::egfp;mitf::xmrk* transgenic medaka, we examined the average number of sprouts and branch points appearing in the area between fin ray hemispheres (Fig. 1D,E). Both were strongly and significantly increased in *fli::egfp;mitf::xmrk* transgenic medakas compared to control fish. We also observed a correlation between the number of transformed cells in caudal fins of *fli::egfp;mitf::xmrk* transgenic medakas and the extent of vessel density (Fig. 1F). Furthermore, it appeared that even single *xmrk*-transformed pigment cells were able to recruit endothelial sprouts (Fig. 1G, asterisks).

We determined the lateral thickness of the caudal fin to be ~100 μm across the fin ray, which is the thickest part of the fin. In the inter-fin-ray area, where *xmrk*-transgenic pigment cells and angiogenic sprouts appear, the lateral thickness is even less (Fig. 1Hi and ii). However, the tissue diffusion limit is ~100–200 μm (Gasparini, 1999) and hypoxia is not expected to occur below this limit. To verify the absence of hypoxia in the affected tissue, we examined the expression of the established medaka hypoxia markers *epo* and *tert* (Yu et al., 2006) in freshly clipped *mitf::xmrk* tailfins by real-time PCR (supplementary material Fig. S1A). As reference, we used control medaka tailfins. As positive control, excised tailfins which were kept under hypoxic conditions for 24 h were used. They were set in relation to excised tailfins cultivated under normoxic conditions for the same timespan. While both markers increased in the hypoxia-treated tailfins, no changes were observed in *mitf::xmrk* tailfins (supplementary material Fig. S1A). In addition, hypoxia was determined by hypoxyprobe treatment and subsequent antibody detection, as described previously (Jopling et al., 2012). Again, excised tailfins which were kept under hypoxic conditions showed strong staining, which was not detected in fins from *mitf::xmrk* fishes (supplementary material Fig. S1B). Thus, we conclude that lack of oxygen supply in the fin is not the driving force of the observed increased angiogenesis.

### NF-κB is activated by Xmrk

To identify angiogenic factors induced by Xmrk, we took advantage of various well-established and characterized *in vitro* systems. In the first cell culture system, the extracellular part of human EGFR (HER) is fused to the intracellular part of Xmrk (mrk), giving rise to the chimeric protein HERmrk. HERmrk (here also called Hm) was introduced into murine melanocytes,

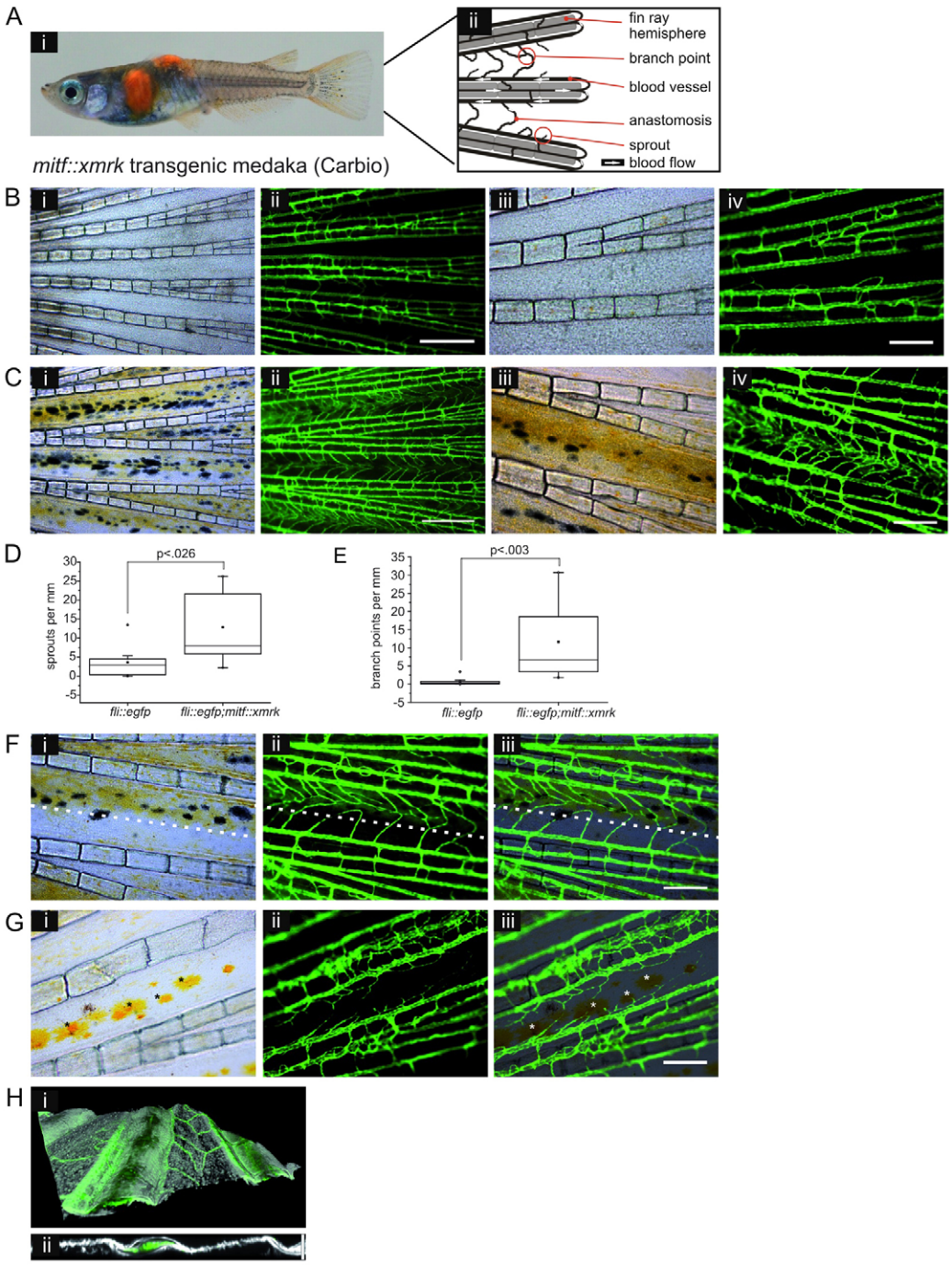


**Fig. 1. Xmrk induces angiogenesis in transgenic *fli::egfp;mitf::xmrk* medaka fishes.** (**A**) Adult *fli::egfp* transgenic medaka (i) and schematic representation of caudal fin blood vessel structure (ii). (**B**) Vessel structure in caudal fins of *fli::egfp* transgenic medaka. (i) Brightfield image and (ii) corresponding GFP fluorescence image at 50-fold magnification. Scale bar: 500 µm. (iii) Brightfield image and (iv) corresponding GFP fluorescence image at 100-fold magnification. Scale bar: 200 µm. (**C**) Vessel structure in caudal fins of *fli::egfp;mitf::xmrk* medaka. (i) Brightfield image and (ii) corresponding GFP fluorescence image at 50-fold magnification. Scale bar: 500 µm. (iii) Brightfield image and (iv) corresponding GFP fluorescence image at 100-fold magnification. Scale bar: 200 µm. (**D**) Average number of inter-fin ray sprouts per mm of fin length in *fli::egfp* and *fli::egfp;mitf::xmrk* transgenic medakas. (**E**) Average number of inter-fin ray vessel branch points per mm of fin length in *fli::egfp* and *fli::egfp;mitf::xmrk* transgenic medakas. Statistical analysis for D and E was carried out using the Mann–Whitney *U* test. Quantification of sprouts and branch points per mm of the inter-fin ray area was performed using seven to eight fish from each group. (**F**,**G**) Caudal fin pigmentation and vascular pattern in *fli::egfp;mitf::xmrk* transgenic medaka. (i) Brightfield image. (ii) Corresponding GFP fluorescence image. (iii) Overlay. Scale bars: 200 µm. White dashed line separates strongly pigmented area of inter fin ray tissue, containing many *xmrk*-expressing cells, from the less pigmented area, containing few *xmrk*-expressing cells. Sprout density is much higher in areas containing a larger number of *xmrk*-expressing pigment cells. (G) Representative image of an area containing few *xmrk*-expressing cells, showing that sprouts are recruited to single transformed pigment cells (asterisks). (i) Brightfield image and (ii) corresponding GFP fluorescence image. (iii) Overlay. Scale bars: 200 µm. (**H**) Confocal image of the caudal fin of a *fli::egfp;mitf::xmrk* medaka. The GFP-positive blood vessels are shown in green, nuclei are depicted in gray (TO-PRO-3 staining). (i) 3D reconstruction of the central part of the caudal fin. (ii) 2D xz plane image, scale bar on the right side of the picture represents 100 µm.

which do not contain endogenous EGFR. In comparison to Xmrk, HERmrk is not constitutively active, but can be stimulated using human EGF. The supernatants of unstimulated as well as EGF-treated HERmrk cells were examined in an ELISA-based angiogenesis array. No differences in expression of well-established angiogenesis inducers like bFGF and VEGF were observed. However, TNF-α, IL-6 and TIMP-1 were slightly induced after HERmrk stimulation (Fig. 2A; supplementary material Fig. S2). All three factors are able to induce pro-angiogenic effects. Even TIMP-1, which was previously considered as anti-angiogenic factor due to its capacity to inhibit matrix metalloproteases, has been recently ascribed pro-tumorigenic and pro-angiogenic roles (Mayrand et al., 2012; Toricelli et al., 2013). Interestingly, TNF-α, IL-6 and TIMP-1 are known targets of NF-κB (Collart et al., 1990; Libermann and Baltimore, 1990; Wilczynska et al., 2006). To find out if NF-κB is activated upon stimulation of HERmrk cells, we analyzed the protein levels of the phosphorylated NF-κB subunit p65 (Ser536) in Hm cells at different time points upon EGF stimulation. Phosphorylation of serine 536 in the transactivation domain 1 of p65 directly indicates DNA binding and transcriptional activity of the NF-κB complex. After 3 and 4 h of EGF stimulation a

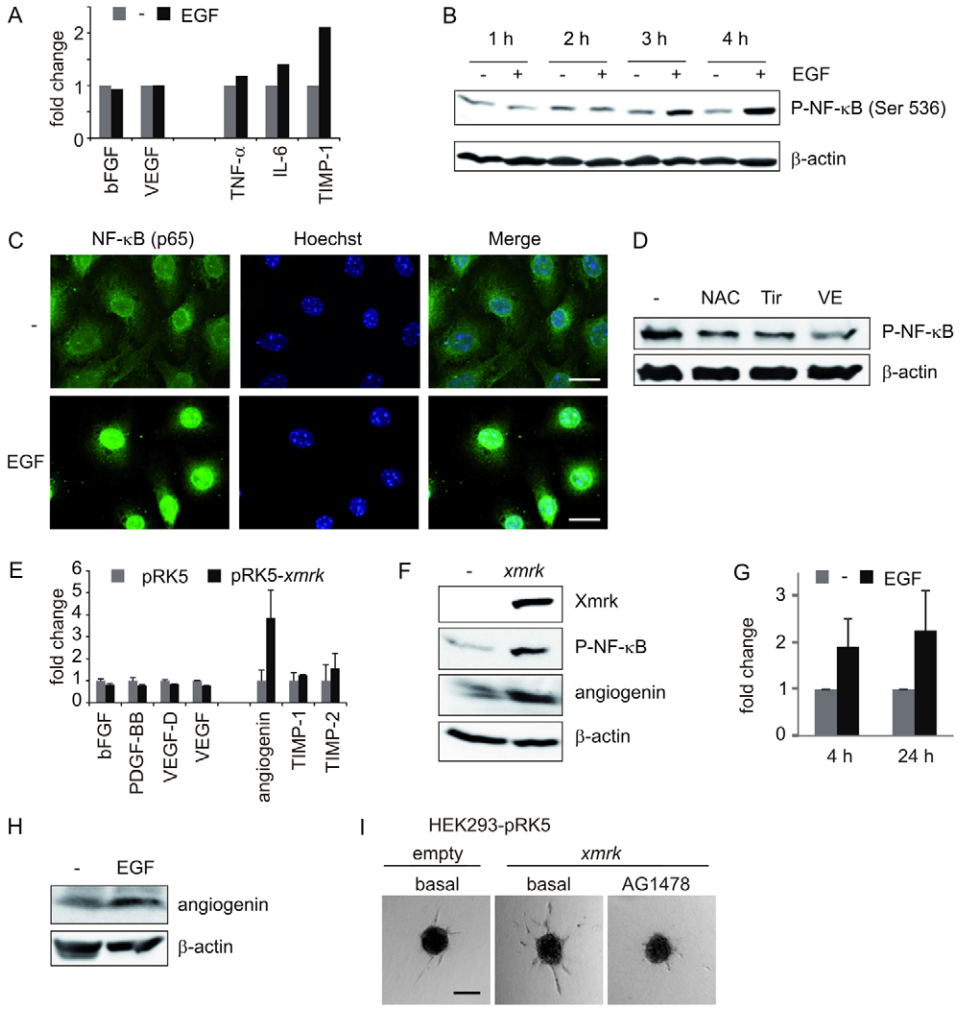


**Fig. 2. Xmrk induces activation of NF-κB and production of angiogenin.** (**A**) Selected graphs from an ELISA-based mouse angiogenesis array of the supernatant from unstimulated (gray bars) and EGF-stimulated (black bars) Hm transgenic melan-a cells. In addition to the well-established angiogenesis inducers bFGF and VEGF, only those proteins that showed an induction after stimulation are displayed. Supernatant from unstimulated cells served as reference and was therefore set to 1. (**B**) Western blot of p65 phospho-NF-κB (Ser536) levels at indicated time points of Hm stimulation. β-Actin served as a loading control. (**C**) Immunfluorescence images illustrating nuclear translocation of NF-κB (p65) after Hm stimulation. NF-κB is displayed in green, the nucleus is shown in blue. (**D**) Phospho-NF-κB (Ser536) protein levels of stimulated Hm cells in the absence of further additives (-), or in presence of 2 mM *N*-acetyl-*L*-cysteine (NAC), 80 µM Tiron (Tir) or 200 µM vitamin E (VE). β-actin served as a loading control. (**E**) Selected graphs from the ELISA-based human angiogenesis array of HEK293-pRK5 (gray bars) and HEK293-pRK5-*xmrk* supernatant (black bars). In addition to the well-established angiogenesis inducers bFGF, PDBF-BB, VEGF-D and VEGF, only those proteins that showed an induction in response to Xmrk are displayed. Supernatant from unstimulated cells served as reference and was therefore set as 1. (**F**) Western blot showing protein levels of Xmrk, phosphorylated NF-κB (Ser536) and angiogenin in HEK293-pRK5 and HEK293-pRK5-*xmrk* cells. β-Actin served as a loading control. (**G**) Real-time PCR analysis showing angiogenin mRNA expression levels of untreated and EGF-stimulated Hm cells after 4 h and 24 h of stimulation. (**H**) Western blot showing protein expression of angiogenin in Hm cells left untreated or stimulated with EGF for 24 h. β-Actin served as a loading control. (**I**) HUVEC spheroid sprouting 24 h after the addition of conditioned supernatant from HEK293 cells stably expressing pRK5 or pRK5-*xmrk*. Where indicated, 10 µM of the EGF receptor inhibitor AG1478 was added. Scale bars: 100 µm.

clear increase of phospho-NF-κB (Ser536) levels was detectable (Fig. 2B). Furthermore, nuclear translocation of total p65 was observed following EGF stimulation (Fig. 2C).

We have previously shown that HERmrk can induce the generation of reactive oxygen species (ROS) (Leikam et al., 2008; Leikam et al., 2013) and that Xmrk-transgenic fish melanomas display a ROS-responsive protein signature (Lokaj et al., 2009). As ROS are potent activators of NF-κB, we investigated their role in NF-κB induction in Hm cells. Application of the ROS scavengers Tiron, N-acetylcysteine (NAC) or vitamin E to EGF-stimulated Hm cells reduced phospho-NF-κB (Ser536) protein levels compared to the EGF-treated control (Fig. 2D). This indicates that HERmrk/Xmrk-generated ROS is capable of enhancing NF-κB activation.

To test the induction of NF-κB and angiogenic factors in a second, independent cell system, we used human HEK293 stably expressing the native oncogenic receptor Xmrk (HEK293-*xmrk* cells). The human-specific angiogenesis array does not entirely overlap with the above used murine array, but it is able to detect additional factors such as VEGF-D, PDGF-BB and angiogenin. Again, no differences between HEK293 control cells and HEK293-*xmrk* cells were visible with respect to the well-established angiogenesis inducers bFGF, VEGF, VEGF-D, or PDGF-BB (Fig. 2E; supplementary material Fig. S3). In contrast to the Hm cell line (Fig. 2A) an induction of TNF-α or IL-6 was not detectable in HEK293 cells. The only proteins which displayed an Xmrk-dependent induction were TIMP1, TIMP2 and, most prominently, angiogenin (Fig. 2E). Like the TIMP proteins, angiogenin is also regulated by NF-κB (Chan et al., 2009). We found that protein levels of both phospho-NF-κB (Ser536) and angiogenin were increased in Xmrk-expressing HEK293 cells in comparison to empty vector transfected control cells (Fig. 2F). Similarly, mRNA and protein expression levels of angiogenin were induced in response to HERmrk stimulation in the murine Hm cell system (Fig. 2G,H).

To investigate if Xmrk expresssion is sufficient to induce endothelial sprouting *in vitro*, we stimulated embedded HUVEC spheroids with supernatants from either control or Xmrk-expressing HEK293 cells (schematically depicted in supplementary material Fig. S4). The supernatant from Xmrk-expressing cells strongly enhanced HUVEC sprouting, and this effect was prevented in presence of the EGFR inhibitor AG1478 which blocks Xmrk activity (Fig. 2I).

### Xmrk-driven enthodelial sprouting is mediated by NF-κB and ROS

As Xmrk expression was sufficient to induce endothelial sprouting *in vitro*, we made use of the sprouting assay to explore the functional effects of ROS and NF-κB-dependent signaling. Control (pRK5) or *xmrk*-transgenic (pRK5-*xmrk*) HEK293 cells were left untreated or were pretreated for 24 h with an NF-κB inhibitor or with the ROS scavenger Tiron before their supernatant was applied to HUVEC spheroids. Standard culture medium (‘basal’) and basal medium containing VEGF, directly applied to the HUVEC spheroids, served as negative and positive controls, respectively. Notably, addition of any of the inhibitors to control HEK293 cells did not affect the extent of HUVEC sprouting by the respective supernatant (Fig. 3A,B). However, while the supernatant from Xmrk-expressing HEK293 cells induced HUVEC sprouting, NF-κB inhibition and Tiron treatment prevented this effect. Similar results were obtained when Xmrk

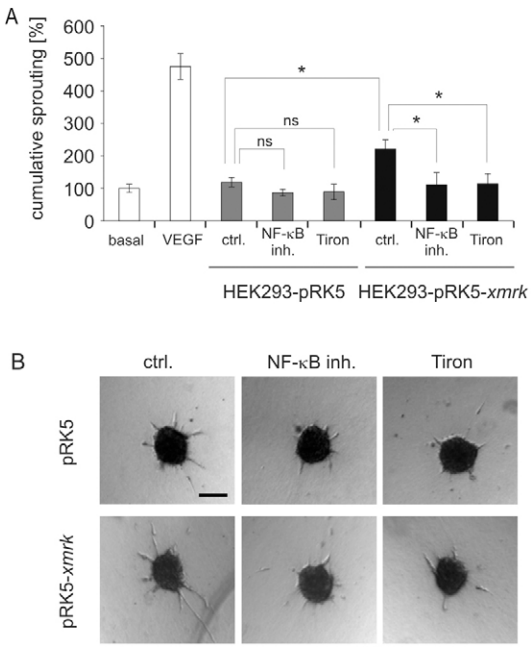


**Fig. 3. Endothelial cell sprouting is mediated by NF-κB and ROS.** (**A**) Cumulative HUVEC sprouting under different conditions. From left to right: basal medium (negative control, set as 100%), basal medium with VEGF (positive control), and supernatants of HEK293 pRK5 cells or HEK293 pRK5-*xmrk* cells. Where indicated, cells were treated for 24 h with DMSO (control), NF-κB inhibitor (10 μM), or Tiron (3 mM), before the supernatant was used for HUVEC stimulation. Statistical analysis was carried out with One Way ANOVA, as post-hoc analysis we used Dunnett’s multiple comparison test. (**B**) Corresponding representative images of HUVEC spheroids after application of indicated cell culture supernatants. Scale bar: 100 μm. *$P<0.05$.

was expressed in the tumor cell line A549 (supplementary material Fig. S5). These results support the assumption that NF-κB and ROS mediate Xmrk-induced angiogenesis.

### NF-κB and ROS mediate angiogenesis *in vivo*

To find out if NF-κB and ROS play a role in hypoxia-independent tumor angiogenesis *in vivo*, we used the *fli::egfp;mitf::xmrk* fish model. One of the prominent advantages of this animal model system is the easy administration of small molecule inhibitors directly to the water of the fish tank. We used age-matched adult *fli::egfp;mitf::xmrk* medakas that were separated into groups of 9–12 fishes. Groups were either treated with DMSO (control group), NF-κB inhibitor or Tiron for one week. Each fish was monitored before and after treatment. DMSO-treated control fishes displayed a slight increase in the number of blood vessel sprouts during one week, but no change of branch points during this time (Fig. 4A–C). NF-κB inhibitor and Tiron, however, led to a degeneration and consequently a significant decrease of preformed sprouts (Fig. 4A,B). Furthermore, there was also a trend towards decreased numbers of branch points in NF-κB- and Tiron-treated fishes, but this did not reach significance (Fig. 4C).

### NF-κB is active in human melanoma cells and induces the production of angiogenin

NF-κB is often activated in human melanoma, where it facilitates tumor invasion and proliferation, prevents apoptosis and induces

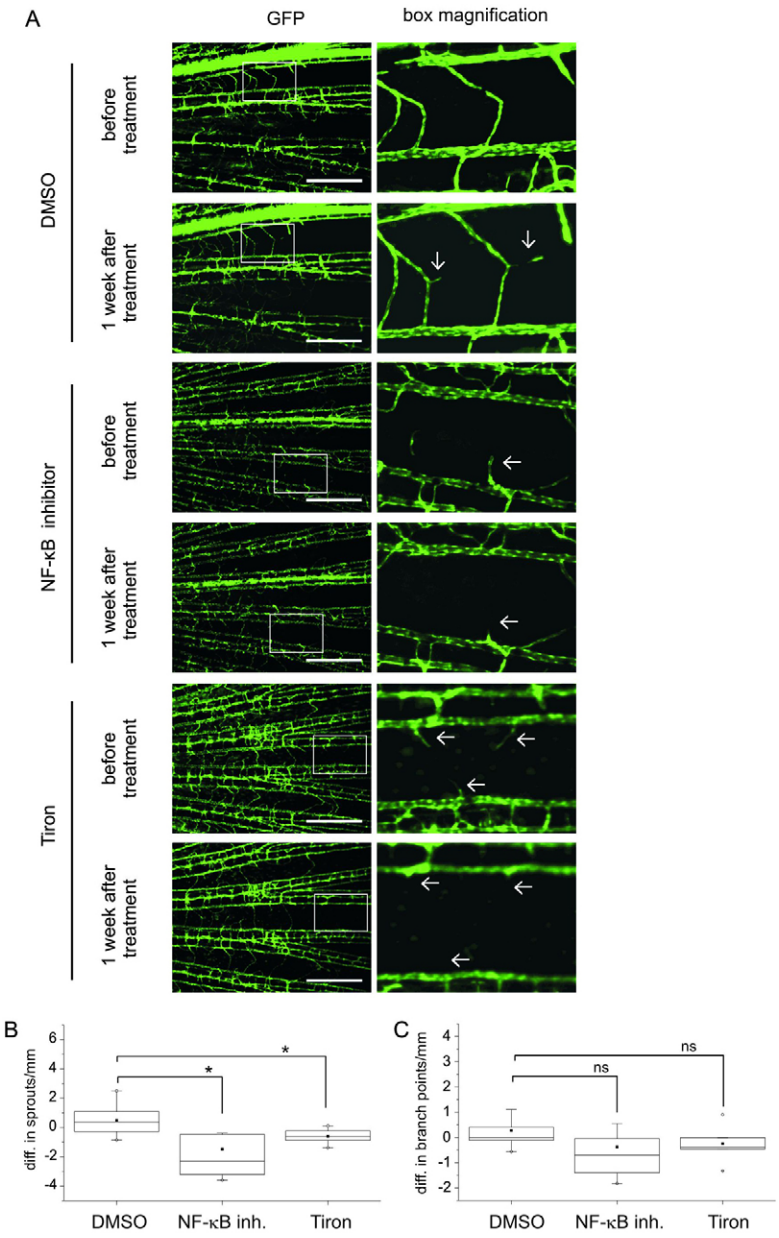


**Fig. 4. NF-κB and ROS mediate Xmrk-dependent angiogenesis *in vivo*.** (**A**) Panels show caudal fins of transgenic *fli::egfp;mitf::xmrk* medaka fishes before treatment and after 1 week of continuous treatment with DMSO, NF-κB inhibitor (100 nM) or Tiron (3 mM). Left panel: overview GFP images; right panel: magnified view of the box indicated on the left. Scale bars: 500 µm. Although the number of sprouts slightly increases after 1 week of DMSO treatment, they disintegrate in response to NF-kB or Tiron, as indicated by the arrows. (**B**) Average difference in the number of sprouts per mm caudal inter-fin-ray area after 1 week of NF-κB inhibitor or Tiron treatment. (**C**) Average difference in the number of branch points per mm caudal inter-fin-ray area after 1 week of NF-κB inhibitor or Tiron treatment. DMSO-treated control fish served as a reference (A–C). Statistical analysis was carried out using the Kruskal–Wallis test. As post-hoc analysis we used an approach based upon the Tukey method as described (Sokal and Rohlf, 1995) (B,C). The data were derived from 12 control fishes, 11 NF-κB-inhibitor-treated fishes and nine Tiron-treated fishes. *$P<0.05$.

angiogenesis (Ueda and Richmond, 2006). To investigate a possible connection between NF-κB and the production of angiogenesis inducers in human melanoma cells, we treated the human melanoma cell line Mel Im with NF-κB inhibitor and performed an ELISA-based angiogenesis array. Mel Im cells were chosen because of their high intrinsic NF-κB activity (Kuphal et al., 2010). Interestingly, only angiogenin, TIMP1, TIMP2 and GRO were downregulated upon NF-κB inhibitor treatment, indicating that these factors are regulated by NF-κB in Mel Im cells (Fig. 5A; supplementary material Fig. S6). Altogether, angiogenin was consistently detected among all cell systems used throughout our experiments. To test the dependence of angiogenin expression on NF-κB signaling in human melanoma cells, we performed inhibitor experiments. Pretreatment of Mel Im cells with NF-κB inhibitor strongly decreased phospho-NF-κB (Ser536) levels, which went along with a reduction of angiogenin protein (Fig. 5B). The same was also true for the other three investigated melanoma cell lines Mel Wei, Mel Ho and A375 (Fig. 5C).

It was previously described that angiogenin is upregulated by hypoxia in some melanoma cell lines (Hartmann et al., 1999). To test if hypoxia, NF-κB, or both are relevant for angiogenin production in the melanoma cell lines used here, Mel Im, Mel Wei and A375 were kept for 24 h under normoxic or hypoxic conditions and in absence or presence of NF-κB inhibitor (Fig. 5D). Subsequently, the protein levels of angiogenin were analyzed. Surprisingly, hypoxia did not lead to an increase, but rather a decrease of angiogenin levels, whereas NF-κB was required for angiogenin expression in all cases except in hypoxia-treated A375 cells. In Xmrk-expressing HEK293 cells, hypoxia had no effect on angiogenin expression at all, whereas NF-κB was the responsible factor for maintaining high levels of angiogenin (Fig. 5E).

To test the pro-angiogenic capacity of the NF-κB targets in human melanoma cells, we performed a sprouting assay with

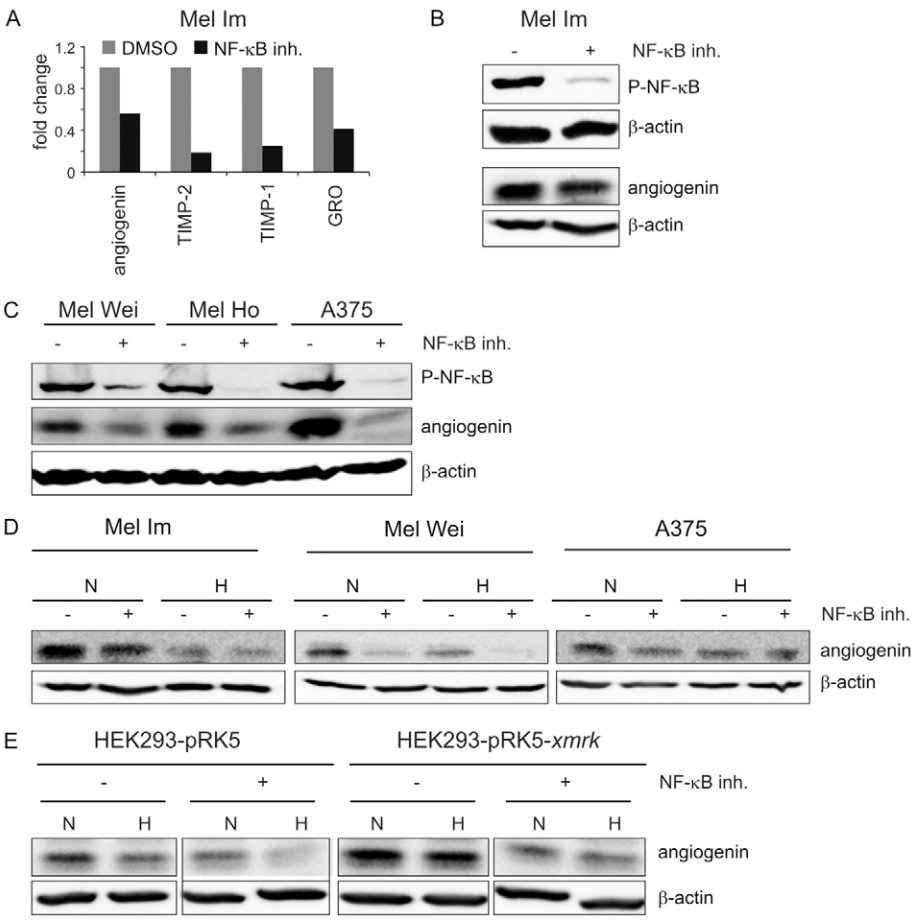


**Fig. 5. Angiogenin is induced upon NF-κB activation in human melanoma cells.** (**A**) Selected graphs from an ELISA-based human angiogenesis array of the supernatant from Mel Im cells pretreated with DMSO (gray bars) or 10 μM of NF-κB inhibitor (black bars). The graph shows the four most strongly regulated proteins. Supernatant from DMSO-treated cells served as a reference and is therefore set as 1. (**B**) Western blot of phosphorylated NF-κB (Ser536) and angiogenin protein levels in Mel Im cells treated with DMSO or NF-κB activation inhibitor (10 μM). (**C**) Western blot of phosphorylated NF-κB (Ser536) and angiogenin protein levels of untreated or NF-κB-inhibitor-treated (10 μM) Mel Wei, Mel Ho and A375 cells. (**D**) Western blots displaying angiogenin protein levels in Mel Im, Mel Wei and A375 cells in the presence or absence of NF-κB inhibitor (10 μM) and under normoxic (N) and hypoxic (H) conditions. (**E**) Protein levels of angiogenin in HEK293-pRK5 or HEK293-pRK5-*xmrk* cells in the presence or absence of 10 μM NF-κB inhibitor and under normoxic (N) and hypoxic (H) conditions. All samples shown in E were analyzed on the same blot, but the arrangement was changed after developing. For all western blots, β-actin served as a loading control.

conditioned supernatant from three different melanoma cell lines treated with control-, angiogenin- and TIMP1-specific siRNA (Fig. 6; supplementary material Fig. S7). The respective siRNA treatment had no effect on cell viability, as measured by MTT assay (Fig. 6A). In contrast, knockdown of angiogenin and TIMP1 reduced the sprouting capacity of the melanoma cell supernatant (Fig. 6B).

In summary, we demonstrate in an experimental melanoma model that angiogenesis can efficiently occur even in absence of hypoxia and is instead regulated by ROS-driven NF-κB activation. Similar processes occur in human melanoma cells, where strong angiogenesis inducers like angiogenin are upregulated by high intrinsic NF-κB activity.

## Discussion

Due to their high transparency and the consequential opportunities for bioimaging analyses, fish models are perfectly suited for angiogenesis research. Tumor- and melanoma angiogenesis were described previously in zebrafish, but in contrast to our model, the common zebrafish angiogenesis models encompass the usage of embryos instead of adult fishes. Typically, human or murine tumor cells are injected into the perivitelline space of zebrafish larve 48–72 h post fertilization (Nicoli and Presta, 2007). Although these models are undoubtedly of high importance, the vascular system is still developing at these early stages, thus increasing the endothelial sensitivity to angiogenic cues. Our model does not have the need for invasive manipulation or the artificial grafting of aggressive tumor cells. Here, hyperpigmentation and the corresponding development of premalignant lesions occur slowly during the lifetime of the individual fish, and the observed angiogenic sprouts appear from fully developed blood vessels. This situation mimics more closely the situation in human patients.

Similar to many other tumor cells, human melanoma cells express a variety of angiogenic factors, such as VEGF, bFGF, PlGF, IL-6 and IL-8 (Mahabeleshwar and Byzova, 2007), Furthermore, matrix metalloproteases (MMP) and certain integrin components such as integrin $\alpha_V\beta_3$ are crucially involved in tumor progression and angiogenesis (Mahabeleshwar and Byzova, 2007) and are also regulated by Xmrk (Geissinger et al., 2002; Meierjohann et al., 2010). Although classical anti-angiogenic strategies such as VEGFR2-, integrin- or MMP inhibition showed a certain effect on angiogenesis and tumor load in mice, their success in humans was very limited due to therapy resistance.

It has been reported that many of the pro-angiogenic factors, such as VEGF and integrin $\alpha_v\beta_3$, are induced by hypoxia (Cowden Dahl et al., 2005; el Filali et al., 2010). Hypoxia-driven VEGF secretion is further potentiated by the activation of classical oncogenes such as RAS or BCL-2, with the involvement of both PI3K and MAPK pathways (Shellman et al., 2003; Trisciuoglio et al., 2005). However, VEGF secretion as well as HIF-1α activation may also occur in an entirely hypoxia-independent manner, e.g. if the von Hippel Lindau (vHL) protein, which is usually involved in the quick degradation of HIF-1α, is deleted or mutated, as often observed in kidney cancer

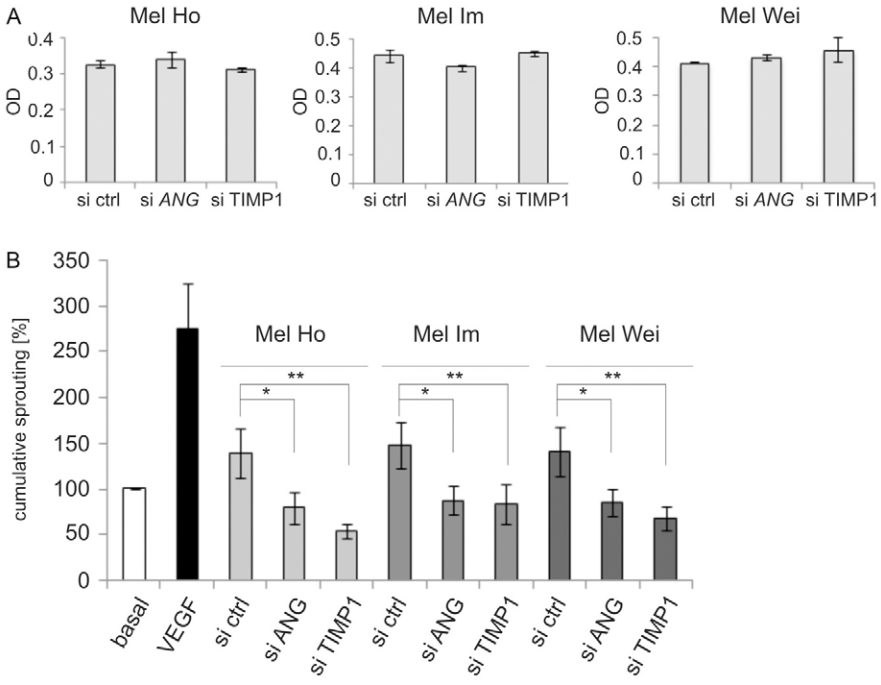


**Fig. 6. The NF-κB targets angiogenin and TIMP1 serve as pro-angiogenic factors in human melanoma cell lines.** (**A**) MTT assay showing the viability of Mel Ho, Mel Im and Mel Wei cell lines after transfection with the control or *ANG*- and *TIMP1*-specific siRNA, respectively. The graph displays the optical density (OD) of the colorimetric product. For knockdown efficiency, see supplementary material Fig. S7. (**B**) Cumulative HUVEC sprouting in the presence of basal medium (negative control, set as 100%), basal medium with VEGF (positive control), and supernatants of the indicated melanoma cell lines Mel Ho, Mel Im and Mel Wei. Cells were transfected with the indicated siRNA 3 days before the supernatant was used for HUVEC stimulation. Statistical analysis was carried out with One Way ANOVA. As post-hoc analysis we used Dunnett's multiple comparison test. $*P<0.05$, $**P<0.01$.

(Cowey and Rathmell, 2009). Interestingly, enhanced AKT kinase signaling as well as ROS also lead to hypoxia-independent HIF-1α stabilization and can thereby induce pro-angiogenic factors (Perry and Arbiser, 2006). In this context, it has been proposed that high intrinsic levels of VEGF and bFGF may be more important than hypoxia-induced upregulation of these factors in the angiogenesis of melanoma xenografts (Rofstad and Mathiesen, 2010).

In line with these observations, we show here for the first time in a transgenic *in vivo* melanoma model that melanoma angiogenesis is very effective *in vivo* even in absence of hypoxia. Instead, angiogenesis is mediated by the NF-κB pathway. As many classical oncogenes such as RAS, AKT, BCR-ABL and receptor tyrosine kinases induce NF-κB signaling, NF-κB is constitutively activated in numerous cancer types, including melanoma, where it is crucially involved in features that are implicated in metastasis, chemoresistance and apoptosis prevention (Ueda and Richmond, 2006). Although hypoxia is a known trigger of NF-κB, we could demonstrate that in all cell lines we investigated, high levels of activated NF-κB were present under normoxic conditions. In melanoma, there are many potential NF-κB stimuli. The tumor suppressor locus CDKN2A is often deleted or mutated in this tumor type, which ablates the inhibitory effect of its gene products INK4A and ARF on NF-κB activity. In addition, constitutively activated MAPK or AKT signaling, mediated through the melanoma oncogenes $BRAF^{V600E}$ or $NRAS^{Q61K}$ as well as mutations in the tumor suppressor PTEN, are known inducers of NF-κB (Ueda and Richmond, 2006).

ROS are also very efficient activators of NF-κB, and an increasing body of evidence implicates that cancer cells in general and melanoma cells in particular display high ROS levels which are required to mediate many of the specific characteristics of tumor cells (Fruehauf and Trapp, 2008). High levels of Xmrk generate a substantial ROS load (Leikam et al., 2008). It is known that EGF receptors, a group of RTKs that includes Xmrk, can mediate ROS induction by activating NADPH oxidases (Browe and Baumgarten, 2006). Here we show that scavenging of ROS by Tiron blocked NF-κB activation, indicating that Xmrk-dependent NF-κB stimulation is mediated by ROS. A link between ROS levels and NF-κB activity was previously demonstrated for human melanoma (Kuphal et al., 2010), and NADPH oxidases in particular are involved in NF-κB activation and melanoma growth (Brar et al., 2002). The potency of ROS as angiogenesis inducer was furthermore revealed in a murine model for retinal neoangiogenesis and tumor angiogenesis induced by melanoma xenografts. Here, the DNA damage sensor kinase ATM proved to be necessary for mediating ROS-induced angiogenesis (Okuno et al., 2012). Interestingly, ATM can enhance NF-κB activity by activating the IκB kinase complex, thereby providing a link between ROS, DNA damage and NF-κB activation (Wu et al., 2006).

Although VEGF-A belongs to the NF-κB targets, its secretion was not modulated by Xmrk in the cell culture model or by NF-κB inhibition in the human melanoma cell line Mel Im, which is characterized by high NF-κB levels (Kuphal et al., 2010). The pro-angiogenic compound angiogenin, however, was strongly secreted in Xmrk-transgenic cells, and NF-κB inhibition of these cells or human melanoma cell lines reduced angiogenin secretion to background levels. In concordance, the angiogenin promoter contains NF-κB binding sites. It was observed previously that advanced melanomas are characterized by high angiogenin expression when compared to nevi (Hartmann et al., 1999). When we investigated angiogenin expression in a set of melanoma samples, we found it to be expressed in 4/10 primary tumors and 5/10 metastases (examples shown in supplementary material Fig. S8). Although our data reveal a weaker melanoma staining compared to Hartmann and colleagues – potentially due to differences in antibody sensitivity or previous patient treatment – the trend towards clearly visible angiogenin expression in melanoma is consistent. Still, our *in vitro* data show that non-transformed melanocytes

also express some angiogenin, as demonstrated for cultivated and unstimulated melan-a HERmrk cells, though HERmrk stimulation further increases this effect (see Fig. 2H). Thus, angiogenin alone is obviously not sufficient to mediate angiogenesis. In comparison to that, the strong angiogenesis inducer NF-κB, which induces additional pro-angiogenic factors besides angiogenin, is a specific characteristic attribute of melanoma, but not nevi (Gao et al., 2006).

The observation that melanoma angiogenesis *in vivo* can be mediated by single transformed cells is both striking and unexpected. A question arising from our data is whether a similar angiogenesis process also occurs in humans, thereby contributing to the poor prognosis of patients with metastasized melanoma. As single metastasized tumor cells outside blood vessels or lymph tissue are below the detection limit in human patients, it is not known if single melanoma cells already have angiogenic potential. Still, the first pro-angiogenic factors are already detected in the radial growth phase (RGP) of cutaneous melanoma (Marcoval et al., 1997). RGP melanomas are below 1 mm in thickness, and they are restricted to the epidermis. Due to the dermal barrier, angiogenesis cannot take place at this stage of the disease, and the secretion of the factors is without effect. However, fully transformed, but thin cutaneous melanomas that are below the proposed hypoxia limit of 1 mm thickness and have overcome the dermal barrier do indeed induce angiogenesis (Barnhill and Levy, 1993). Thus, the pro-angiogenic capacity of a tumor is not necessarily dependent on hypoxia, but on the malignancy of the cell. This hypothesis is supported by results from injections of melanoma cells of different malignancy into *flk1::egfp*-transgenic zebrafish embryos. 100–300 non-metastatic B16 mouse melanoma cells were necessary to induce angiogenesis, whereas the metastatic melanoma cell line B16-F10 required only 15–30 cells to induce an angiogenic response (Zhao et al., 2011). The angiogenesis-inducing capacity of melanoma cells thus seems to depend on their ability to initiate and maintain a pro-angiogenic signaling threshold. Xmrk-transformed pigment cells and probably also human melanoma cells are able to keep up such a high signaling threshold. In conclusion, the pharmacological targeting of multi-potent signaling pathways with angiogenesis-dependent as well as -independent pro-tumorigenic effects such as the NF-κB pathway might be a promising anti-tumor strategy.

## Materials and Methods

### Fish maintenance and generation of the melanoma angiogenesis model

Fishes were maintained under standard conditions with an artificial photoperiod (10 hours of darkness, 14 hours of light). For all assays, fishes were kept in a medium containing 17.4 mM NaCl, 210 µM KCl, 180 µM $Ca(NO_3)_2$, 120 µM $MgSO_4$, 1.5 mM HEPES. To allow *in vivo* observation of the vasculature a transgenic line was produced that expresses enhanced GFP (EGFP) under control of the zebrafish *fli1* 15 kb regulatory region (Lawson and Weinstein, 2002). Plasmid pfli15EGFP, kindly supplied by Dr B. Weinstein, was injected into one cell stage medaka embryos of the Cab strain using standard procedures (see Patton et al., 2011), except that 0.5 SceI buffer was used as injection fluid. Stable lines were established by crossing positive founder fish to Cab strain medaka. Transgenic fish lines *mitf::xmrk* (Schartl et al., 2010) and *fli::egfp* were crossed to generate *fli::egfp;mitf::xmrk* double transgenic fishes. Quantification of sprouts and branch points per mm inter-fin ray area was performed using at least seven fishes from each group. All animal studies have been approved by the author's institutional review board (Animal Welfare Officer of the University of Wurzburg).

### Cell culture

Mouse melanocytes transfected with HERmrk (melan-a Hm) were cultured as described previously (Leikam et al., 2008). For small molecular inhibitor experiments, Hm cells were starved for 3 days in 2,5% starving medium [Dulbecco's Modified Eagle's Medium (DMEM) supplemented with penicillin (400 U/ml), streptomycin (50 µg/ml) and 2.5% dialyzed fetal calf serum (FCS, Invitrogen)]. Inhibitors were applied at indicated concentrations. One hour after inhibitor treatment, cells were stimulated with 100 nM human EGF (hEGF). Human embryonic kidney cells HEK293 and adenocarcinoma-derived human alveolar basal epithelial cells (A549), transfected with pRK5 or pRK5-xmrk were maintained in DMEM supplemented with penicillin (400 U/ml), streptomycin (50 µg/ml), and 10% fetal calf serum (FCS, Invitrogen). Human melanoma cell lines Mel Im, Mel Wei, Mel Ho and A375 were maintained in DMEM supplemented with penicillin (400 U/ml), streptomycin (50 µg/ml), L-glutamine (300 µg/ml) and 10% FCS (Invitrogen). Human umbilical vein endothelial cells were cultured in ECGM2 with SupplementMix (PromoCell) and 10% FCS (Biochrom). Hypoxia experiments were performed at 1% $O_2$ (Pro-Ox controller, Biospherix, USA).

### siRNA transfection

Commercially available control siRNA and siRNA against human *ANG* or *TIMP1* (Smart Pool On Target Plus, Thermo Scientific) were transfected using X-treme gene transfection reagent (Roche), according to the manufacturer's recommendations. Cells were analyzed 3 days after transfection. To generate the conditioned medium, the cells were transferred to Endopan medium (PAN Biotech) 1 day after siRNA transfection.

### Cell viability assay

Cell viability was assessed using MTT [3-(4,5-dimethylthiazol-2-yl)-2,5-diphenyltetrazolium bromide] staining (Sigma-Aldrich), as described by the manufacturer. Briefly, cells were transfected with the indicated siRNA and were seeded the following day at a density of $4\times10^3$ cells per well into a 96-well plate. After adhesion, medium was replaced by Endopan medium (PAN Biotech). After 48 h, 5 mg/ml MTT was added and incubated for 2 h at 37℃. The supernatant was removed and reaction products were solubilized for 1 h in DMSO. Absorbance was measured at 570 nm with a reference wavelength of 650 nm using an ELISA reader (Sunrise Absorbance Reader, Tecan). Each experimental condition was analyzed in quadruplicate.

### *In vivo* inhibitor treatment

For the *in vivo* treatment of transgenic *fli::egfp;mitf::xmrk* and *fli::egfp* medakas, 100 nM NF-κB activation inhibitor (Calbiochem) or 3 mM Tiron (dissolved in DMSO) were administered for the indicated timespan. The tank water including inhibitors was exchanged every second day. DMSO treatment served as control. Quantification of sprouts and branch points per mm inter-fin ray area was performed using at least nine fishes from each group.

### Microscopy

For imaging, fishes were anesthetized with a 1:2000 dilution of pure 2-phenoxyethanol. Pictures were taken with a Leica DMI6000 B microscope. Leica Application Suite (LAS) Microscope Software and ImageJ software were used to analyze the raw data.

For confocal microscopy the caudal fins of transgenic *fli::egfp;mitf::xmrk* medakas were cut and fixed in 4% paraformaldehyde in phosphate buffered saline (PBS) over night. After three washing steps with PBS fins were gradually dehydrated with increasingly concentrated methanol solution (up to 100%) and incubated at room temperature overnight. Subsequently, fins were gradually hydrated with PBS and were incubated for 1 hour with the TO-PRO-3 DNA stain (1:1000, Invitrogen). After three washing steps with PBS, fins were incubated in PBS overnight at room temperature. Fins were then transferred to glass slides and were covered with Mowiol® 4-88 (Roth). Images were captured with a Nikon C2 confocal microscope.

### Gene expression analysis

Hm cells were starved for 3 days in 2.5% starving medium and were subsequently stimulated with 100 ng/ml hEGF for indicated times. All other cell lines were treated as indicated in the figure legends. RNA extraction from stimulated Hm cells and human cell lines was done using Total RNA Isolation Reagent (ABGene) as recommended by the manufacturer. cDNA was prepared from total RNA using the RevertAidTM First Strand cDNA Synthesis Kit with random hexamer primers (Fermentas). PCR primers (supplementary material Table S1) were designed using Primer-Blast (http://www.ncbi.nlm.nih.gov/tools/primer-blast/). PCR was carried out using the Eppendorf Mastercycler® ep realplex thermal cycler. Values for each gene were normalized to expression levels of β-actin. Relative expression levels were calculated applying REST software. The data represent the results from two different biological replicates that were each analyzed by three independent realtime PCRs.

### Cell lysis and western blot analysis

Shortly, 50 µg of each protein lysate was seperated by SDS–PAGE and analysed by immunoblotting. Polyclonal anti-Xmrk antiserum was generated by Biogenes.

Anti-β-actin (C-4) and Anti-ANG-I (C-1) antibodies were purchased from Santa Cruz Biotechnology. Anti-P-NF-κB-p65 (Ser536) (93H1) antibody was purchased from Cell Signaling Technology (New England Biolabs). Secondary antibodies were conjugated to horseradish peroxidase and were directed against mouse (Pierce, Rockford, IL) and rabbit (Bio-Rad). Images were acquired with KODAK image station.

### Spheroid sprouting assay

This assay was performed as described before (Brütsch et al., 2010; Wüstehube et al., 2010). Shortly, human umbilical vein endothelial cells (HUVECs) were trypsinized and suspended in growth medium with 20% Methocel (Sigma-Aldrich). 25 µl drops were put on a culture dish lid and incubated as hanging drops for 24 h to form spheroids containing ca. 400 cells each. Spheroids were suspended in 2 ml Methocel with 20% FCS and 2 ml rat collagen and embedded in a 24-well plate. 0.1 ml basal culture medium was added to assess basal sprouting, while 25 ng/ml VEGF was added for stimulation where indicated. Alternatively, conditioned medium from control or *xmrk*-transgenic HEK293 or A549 cells or from siRNA-treated human melanoma cells Mel Ho, Mel Im or Mel Wei was added. After 24 h collagen beds were fixed with 10% formaldehyde. The lengths of all sprouts of at least 10 spheroids per condition were counted using an inverted microscope (Olympus IX50 with cell/^P software). Each experiment was performed three times.

### Pathway analysis

For the identification of pathways which regulate the expression of candidate genes *in vitro*, we added the following small molecule inhibitors in the indicated concentration to the cell culture medium or spheroid supernatant: AG1478 (inhibitor of EGFR and Xmrk), Tiron (*4,5*-dihydroxy-*1,3*-benzenedisulfonic acid disodium salt monohydrate; scavenger of reactive oxygen species), *N*-acetyl-*L*-cysteine, NF-κB activation inhibitor and Vitamin E (α-tocopherol), respectively. Cells without small molecule inhibitor treatment received the equivalent amount of solvent.

### Immunofluorescence

Hm cells were seeded on glass coverslips, starved for 3 days in DMEM with 2.5% dialyzed FCS. Cells were then stimulated with 100 ng/ml EGF for 24 h or remained unstimulated. Immunofluorescence was performed as described before (Leikam et al., 2008). Anti-NF-κB p65 (E498) antibody (1:100; Cell Signaling) and Alexa Fluor 488 goat anti-rabbit IgG (1:1000; Invitrogen) were used. For nuclear staining, 1 µg/ml of Hoechst 34580 (Invitrogen) was used.

### Angiogenesis array

Mouse and human angiogenesis arrays were purchased from RayBio®. All cell lines were seeded at a density of $1\times10^6$ cells per 10 cm dish and were incubated in a total volume of 7 ml DMEM media with or without 10 µM of NF-κB activation inhibitor (Invitrogen). After 24 h, 2 ml of non-concentrated supernatant of each conditioned medium was used for the assay. Assays were done as recommended by the manufacturer's protocol.

## Acknowledgements

We would like to thank Anita Hufnagel for excellent technical assistance. We are also grateful to Katja Maurus and Susanne Kneitz for their help with the hypoxia measurement and statistical analyses, respectively.

## Author contributions

M.K.S. performed experiments, analyzed data and wrote parts of the manuscript; W.-J.Y. performed and analyzed sprouting assays; L.C. and J.W. created and supplied *fli::egfp* fish; A.B. provided the IHCs and discussed data; A.F. provided expertise and designed the sprouting assays; M.S. provided expertise, discussed the data and contributed to writing the manuscript; S.M. designed the project, analyzed data and wrote the manuscript.

## Funding

This work was supported by the Deutsche Forschungsgemeinschaft [grant number SFB-487 to M.K.S., M.S., S.M.]; the Melanoma Research Network of the Deutsche Krebshilfe e.V. (German Cancer Aid) (to M.S., S.M., A.B.); the Cooperation Program in Cancer Research of the Deutsches Krebsforschungszentrum (DKFZ) and Israel's Ministry of Science and Technology (MOST); and Deutsche Forschungsgemeinschaft [grant number SFB-TR23 to A.F.].

Supplementary material available online at
http://jcs.biologists.org/lookup/suppl/doi:10.1242/jcs.125021/-/DC1

## References

**Barnhill, R. L. and Levy, M. A.** (1993). Regressing thin cutaneous malignant melanomas (< or = 1.0 mm) are associated with angiogenesis. *Am. J. Pathol.* **143**, 99-104.

**Brar, S. S., Kennedy, T. P., Sturrock, A. B., Huecksteadt, T. P., Quinn, M. T., Whorton, A. R. and Hoidal, J. R.** (2002). An NAD(P)H oxidase regulates growth and transcription in melanoma cells. *Am. J. Physiol.* **282**, C1212-C1224.

**Browe, D. M. and Baumgarten, C. M.** (2006). EGFR kinase regulates volume-sensitive chloride current elicited by integrin stretch via PI-3K and NADPH oxidase in ventricular myocytes. *J. Gen. Physiol.* **127**, 237-251.

**Brütsch, R., Liebler, S. S., Wüstehube, J., Bartol, A., Herberich, S. E., Adam, M. G., Telzerow, A., Augustin, H. G. and Fischer, A.** (2010). Integrin cytoplasmic domain-associated protein-1 attenuates sprouting angiogenesis. *Circ. Res.* **107**, 592-601.

**Chan, D. A., Kawahara, T. L., Sutphin, P. D., Chang, H. Y., Chi, J. T. and Giaccia, A. J.** (2009). Tumor vasculature is regulated by PHD2-mediated angiogenesis and bone marrow-derived cell recruitment. *Cancer Cell* **15**, 527-538.

**Collart, M. A., Baeuerle, P. and Vassalli, P.** (1990). Regulation of tumor necrosis factor alpha transcription in macrophages: involvement of four kappa B-like motifs and of constitutive and inducible forms of NF-kappa B. *Mol. Cell. Biol.* **10**, 1498-1506.

**Cowden Dahl, K. D., Robertson, S. E., Weaver, V. M. and Simon, M. C.** (2005). Hypoxia-inducible factor regulates alphavbeta3 integrin cell surface expression. *Mol. Biol. Cell* **16**, 1901-1912.

**Cowey, C. L. and Rathmell, W. K.** (2009). VHL gene mutations in renal cell carcinoma: role as a biomarker of disease outcome and drug efficacy. *Curr. Oncol. Rep.* **11**, 94-101.

**Dutcher, J. P.** (2001). Angiogenesis and melanoma. *Curr. Oncol. Rep.* **3**, 353-358.

**el Filali, M., Missotten, G. S., Maat, W., Ly, L. V., Luyten, G. P., van der Velden, P. A. and Jager, M. J.** (2010). Regulation of VEGF-A in uveal melanoma. *Invest. Ophthalmol. Vis. Sci.* **51**, 2329-2337.

**Folkman, J.** (2000). Incipient angiogenesis. *J. Natl. Cancer Inst.* **92**, 94-95.

**Fruehauf, J. P. and Trapp, V.** (2008). Reactive oxygen species: an Achilles' heel of melanoma? *Expert Rev. Anticancer Ther.* **8**, 1751-1757.

**Gao, K., Dai, D. L., Martinka, M. and Li, G.** (2006). Prognostic significance of nuclear factor-kappaB p105/p50 in human melanoma and its role in cell migration. *Cancer Res.* **66**, 8382-8388.

**Gasparini, G.** (1999). The rationale and future potential of angiogenesis inhibitors in neoplasia. *Drugs* **58**, 17-38.

**Geissinger, E., Weisser, C., Fischer, P., Schartl, M. and Wellbrock, C.** (2002). Autocrine stimulation by osteopontin contributes to antiapoptotic signalling of melanocytes in dermal collagen. *Cancer Res.* **62**, 4820-4828.

**Hartmann, A., Kunz, M., Köstlin, S., Gillitzer, R., Toksoy, A., Bröcker, E. B. and Klein, C. E.** (1999). Hypoxia-induced up-regulation of angiogenin in human malignant melanoma. *Cancer Res.* **59**, 1578-1583.

**Jopling, C., Suñé, G., Faucherre, A., Fabregat, C. and Izpisua Belmonte, J. C.** (2012). Hypoxia induces myocardial regeneration in zebrafish. *Circulation* **126**, 3017-3027.

**Kuphal, S., Winklmeier, A., Warnecke, C. and Bosserhoff, A. K.** (2010). Constitutive HIF-1 activity in malignant melanoma. *Eur. J. Cancer* **46**, 1159-1169.

**Lawson, N. D. and Weinstein, B. M.** (2002). In vivo imaging of embryonic vascular development using transgenic zebrafish. *Dev. Biol.* **248**, 307-318.

**Lee, B. L., Kim, W. H., Jung, J., Cho, S. J., Park, J. W., Kim, J., Chung, H. Y., Chang, M. S. and Nam, S. Y.** (2008). A hypoxia-independent up-regulation of hypoxia-inducible factor-1 by AKT contributes to angiogenesis in human gastric cancer. *Carcinogenesis* **29**, 44-51.

**Leikam, C., Hufnagel, A., Schartl, M. and Meierjohann, S.** (2008). Oncogene activation in melanocytes links reactive oxygen to multinucleated phenotype and senescence. *Oncogene* **27**, 7070-7082.

**Leikam, C., Hufnagel, A., Walz, S., Kneitz, S., Fekete, A., Müller, M. J., Eilers, M., Schartl, M. and Meierjohann, S.** (2013). Cystathionase mediates senescence evasion in melanocytes and melanoma cells. *Oncogene*.

**Libermann, T. A. and Baltimore, D.** (1990). Activation of interleukin-6 gene expression through the NF-kappa B transcription factor. *Mol. Cell. Biol.* **10**, 2327-2334.

**Lokaj, K., Meierjohann, S., Schütz, C., Teutschbein, J., Schartl, M. and Sickmann, A.** (2009). Quantitative differential proteome analysis in an animal model for human melanoma. *J. Proteome Res.* **8**, 1818-1827.

**Mahabeleshwar, G. H. and Byzova, T. V.** (2007). Angiogenesis in melanoma. *Semin. Oncol.* **34**, 555-565.

**Marcoval, J., Moreno, A., Graells, J., Vidal, A., Escribà, J. M., Garcia-Ramírez, M. and Fabra, A.** (1997). Angiogenesis and malignant melanoma. Angiogenesis is related to the development of vertical (tumorigenic) growth phase. *J. Cutan. Pathol.* **24**, 212-218.

**Mayrand, D., Laforce-Lavoie, A., Larochelle, S., Langlois, A., Genest, H., Roy, M. and Moulin, V. J.** (2012). Angiogenic properties of myofibroblasts isolated from normal human skin wounds. *Angiogenesis* **15**, 199-212.

**Meierjohann, S., Hufnagel, A., Wende, E., Kleinschmidt, M. A., Wolf, K., Friedl, P., Gaubatz, S. and Schartl, M.** (2010). MMP13 mediates cell cycle progression in melanocytes and melanoma cells: in vitro studies of migration and proliferation. *Mol. Cancer* **9**, 201.

**Nicoli, S. and Presta, M.** (2007). The zebrafish/tumor xenograft angiogenesis assay. *Nat. Protoc.* **2**, 2918-2923.

**Nicoli, S., Ribatti, D., Cotelli, F. and Presta, M.** (2007). Mammalian tumor xenografts induce neovascularization in zebrafish embryos. *Cancer Res.* **67**, 2927-2931.

**Okuno, Y., Nakamura-Ishizu, A., Otsu, K., Suda, T. and Kubota, Y.** (2012). Pathological neoangiogenesis depends on oxidative stress regulation by ATM. *Nat. Med.* [Epub ahead of print] doi: 10.1038/nm.2846.

**Patton, E. E., Mathers, M. E. and Schartl, M.** (2011). Generating and analyzing fish models of melanoma. *Methods Cell Biol.* **105**, 339-366.

**Perry, B. N. and Arbiser, J. L.** (2006). The duality of angiogenesis: implications for therapy of human disease. *J. Invest. Dermatol.* **126**, 2160-2166.

**Rofstad, E. K. and Mathiesen, B.** (2010). Metastasis in melanoma xenografts is associated with tumor microvascular density rather than extent of hypoxia. *Neoplasia* **12**, 889-898.

**Schartl, M., Wilde, B., Laisney, J. A., Taniguchi, Y., Takeda, S. and Meierjohann, S.** (2010). A mutated EGFR is sufficient to induce malignant melanoma with genetic background-dependent histopathologies. *J. Invest. Dermatol.* **130**, 249-258.

**Shellman, Y. G., Park, Y. L., Marr, D. G., Casper, K., Xu, Y., Fujita, M., Swerlick, R. and Norris, D. A.** (2003). Release of vascular endothelial growth factor from a human melanoma cell line, WM35, is induced by hypoxia but not ultraviolet radiation and is potentiated by activated Ras mutation. *J. Invest. Dermatol.* **121**, 910-917.

**Sokal, R. R. and Rohlf, H. A.** (1995). *Biometry: The Principles and Practice of Statistics in Biological Research*. New York, NY: W. H. Freeman.

**Staton, C. A., Reed, M. W. and Brown, N. J.** (2009). A critical analysis of current in vitro and in vivo angiogenesis assays. *Int. J. Exp. Pathol.* **90**, 195-221.

**Stoletov, K., Montel, V., Lester, R. D., Gonias, S. L. and Klemke, R.** (2007). High-resolution imaging of the dynamic tumor cell vascular interface in transparent zebrafish. *Proc. Natl. Acad. Sci. USA* **104**, 17406-17411.

**Toricelli, M., Melo, F. H., Peres, G. B., Silva, D. C. and Jasiulionis, M. G.** (2013). Timp1 interacts with beta-1 integrin and CD63 along melanoma genesis and confers anoikis resistance by activating PI3-K signaling pathway independently of Akt phosphorylation. *Mol. Cancer* **12**, 22.

**Trisciuoglio, D., Iervolino, A., Zupi, G. and Del Bufalo, D.** (2005). Involvement of PI3K and MAPK signaling in bcl-2-induced vascular endothelial growth factor expression in melanoma cells. *Mol. Biol. Cell* **16**, 4153-4162.

**Ueda, Y. and Richmond, A.** (2006). NF-kappaB activation in melanoma. *Pigment Cell Res.* **19**, 112-124.

**Warren, B. A. and Shubik, P.** (1966). The growth of the blood supply to melanoma transplants in the hamster cheek pouch. *Lab. Invest.* **15**, 464-478.

**Wilczynska, K. M., Gopalan, S. M., Bugno, M., Kasza, A., Konik, B. S., Bryan, L., Wright, S., Griswold-Prenner, I. and Kordula, T.** (2006). A novel mechanism of tissue inhibitor of metalloproteinases-1 activation by interleukin-1 in primary human astrocytes. *J. Biol. Chem.* **281**, 34955-34964.

**Wu, Z. H., Shi, Y., Tibbetts, R. S. and Miyamoto, S.** (2006). Molecular linkage between the kinase ATM and NF-kappaB signaling in response to genotoxic stimuli. *Science* **311**, 1141-1146.

**Wüstehube, J., Bartol, A., Liebler, S. S., Brütsch, R., Zhu, Y., Felbor, U., Sure, U., Augustin, H. G. and Fischer, A.** (2010). Cerebral cavernous malformation protein CCM1 inhibits sprouting angiogenesis by activating DELTA-NOTCH signaling. *Proc. Natl. Acad. Sci. USA* **107**, 12640-12645.

**Yu, R. M., Chen, E. X., Kong, R. Y., Ng, P. K., Mok, H. O. and Au, D. W.** (2006). Hypoxia induces telomerase reverse transcriptase (TERT) gene expression in non-tumor fish tissues in vivo: the marine medaka (Oryzias melastigma) model. *BMC Mol. Biol.* **7**, 27.

**Zhao, C., Yang, H., Shi, H., Wang, X., Chen, X., Yuan, Y., Lin, S. and Wei, Y.** (2011). Distinct contributions of angiogenesis and vascular co-option during the initiation of primary microtumors and micrometastases. *Carcinogenesis* **32**, 1143-1150.